JOURNAL OF MATERIALS SCIENCE 23 (1988) 694–698

Crystallization of potassium titanate from the amorphous phase

TADASHI ENDO, HIROYUKI NAGAYAMA, TSUGIO SATO, MASAHIKO SHIMADA
Department of Applied Chemistry, Faculty of Engineering, Tohoku University, Aoba, Sendai 980, Japan

By using amorphous potassium titanates as the starting materials, a sintered body of $K_2Ti_4O_9$ or $K_2Ti_6O_{13}$ with porous and fibrous textures was prepared. $K_2Ti_2O_5$ and a new phase, $K_6Ti_4O_{11}$ were synthesized by the thermal reaction of KNO_3 with TiO_2 at 1000° C for 10 to 20 h. On leaching in water to expel excess of potassium ions, both phases became amorphous. After mixing and moulding these amorphous materials in the desired proportion, a sintered body containing fibrous crystals of $K_2Ti_4O_9$ was readily fabricated by heating at 1000° C for 12 h. When $\sim$5 wt% B_2O_3 was added to the amorphous phases, single phase $K_2Ti_6O_{13}$, with a fibrous texture grew well on heating at 1000° C for 12 h. Addition of PVA polymer to the amorphous phases was responsible for controlling the porosity of the sintered body, e.g. about 52% theoretical density at 20 wt% PVA polymer. The optimum conditions for preparing the amorphous phases were systematically examined and the effect of the chemical reaction environments, such as different crucible materials on the calcination of KNO_3 and TiO_2, were also discussed.

1. Introduction

Fibrous crystals of alkali titanate, chemical formula $K_2O\ nTiO_2$ ($n = 4, 6$), were found to exhibit superior heat insulation, heat resistance and chemical resistance to corrosion properties, and numerous applications have been widely developed. Calcination [1], flux [2], hydrothermal [3] and melting [4] methods may be used to prepare the well grown fibrous crystals. In most of these synthetic experiments, the crystallization process is governed by the reaction of K_2CO_3 with TiO_2. However, recently we reported that the reaction of TiO_2 with KNO_3 facilitated the formation of $K_2Ti_6O_{13}$ in the fibrous form [5]. In addition, it was found that the amorphous phase was frequently prepared under the reaction conditions for the alkali-rich side in the KNO_3–TiO_2 systems. These experimental results were convincingly confirmed on comparing them with the experimental data reported by Shimizu *et al.* [6], who studied crystallization from the amorphous phase under hydrothermal conditions.

It was difficult to fabricate a sintered body having the texture piled and intertwined with fibrous crystals, because fibrous crystals became orientated along the elongated axis and adhered to each other during the conventional dispersion processing. In the present study, the crystallization and sintering of potassium titanates were investigated using the amorphous phases as the starting materials. As a result, a sintered body of $K_2Ti_4O_9$ or $K_2Ti_6O_{13}$ containing fibrous crystals and having a high porosity, was prepared by addition of B_2O_3 and PVA polymer. It is expected that the sintered body having such a texture would be suitable for the application of fibre-reinforced plastic and metal.

2. Experimental procedure

KNO_3 and TiO_2 (anatase) were intimately mixed in the desired proportion and placed in a platinum or alumina crucible. The mixture was subjected to 1000° C for 4 to 20 h in air. The recovered sample was identified using an X-ray powder diffractometer with Cu$K\alpha$ radiation. The sample was then leached in water for 1/2 to 1 day, filtered and dried at 100° C. After dissolving the sample in hot H_2SO_4 solution and diluting with distilled water, its chemical composition was determined by atomic absorption spectrophotometric analysis for K^+ and Al^{3+}, and calorimetric analysis of $H_2O_2^+$ complex for Ti^{4+}.

Subsequently, the resulting sample was moulded under a loading pressure of 50 to 300 MPa. By heating at 1000° C for 3 to 20 h, a sintered sample was obtained. On adding a desirable proportion of PVA (poly vinyl alcohol) and B_2O_3 to the sample, the same experimental procedure mentioned above was used to fabricate the sintered sample. X-ray powder diffraction and SEM observations of the sintered samples were carried out. The relative density of the sintered sample was measured by a conventional Archimedes' method. TG–DTA was used to investigate the thermal behaviour of the sample, e.g. the nucleation and crystal growth from the amorphous phases.

3. Results and discussion

3.1. Synthesis of amorphous phase

Reaction of KNO_3 with TiO_2 (Anatase) was carried in

0022–2461/88 $03.00 + .12

TABLE I X-ray powder diffraction data of $K_6Ti_4O_{11}$

d(nm)	I	d(nm)	I
0.708	VS	0.284	M
0.696	S	0.278	M
0.585	S	0.275	W
0.323	M	0.271	M
0.318	M	0.269	W
0.315	M	0.248	M
0.301	W	0.230	M
0.296	S	0.218	VW
0.294	M	0.199	W
0.291	W	0.194	W

VS, very strong; S, strong; M, medium; W, weak; VW, very weak.

a platinum crucible at 1000° C in air after mixing intimately in the molar ratios K/Ti = 1 and 3/2, the products of which were white (sample A) and reddish brown (sample B) in colour, respectively. From the X-ray powder diffraction patterns, sample A was identified as $K_2Ti_2O_5$. On the other hand, sample B was a hygroscopic crystalline phase which could not be identified as any potassium titanate reported hitherto. From the results of chemical analysis, the chemical composition of sample B was determined to be $K_6Ti_4O_{11}$. The X-ray diffraction data of sample B are listed in Table I.

In humid air, some reflection peaks tended to shift gradually towards the lower angle and broaden in shape. A study of the precious crystal structure is now under way, and the data will be reported elsewhere.

After leaching in water for 1/2 to 1 day, both phases were readily converted to the amorphous phases, judging from the X-ray powder diffraction pattern. When an alumina crucible was used, $K_2Ti_2O_5$, $K_6Ti_4O_{11}$ and K_3AlO_3 were recognized to coexist. By leaching in water, the K_3AlO_3 phase was rapidly washed out and the amorphous phases were formed.

3.2. Characterization of amorphous phases

Amorphous phases obtained from $K_6Ti_4O_{11}$ prepared in a platinum crucible and from the mixed phases of $K_2Ti_2O_5$ and $K_6Ti_4O_{11}$ prepared in an Al_2O_3 crucible are denoted sample I and sample II, respectively.

With an increasing amount of H_2O supplied for leaching, the K/Ti molar ratio of both the amorphous phases gradually decreased and reached a constant value of 0.5, which corresponded to the apparent chemical formula $K_2Ti_4O_9$.

Fig. 1 shows the TG–DTA curves of (a) sample B, (b) sample I and (c) sample II. The profile of TG–DTA curve (a) was evaluated by comparing with the data of $K_2Ti_2O_5$ reported previously [7]. The two endothermic peaks at 840 and 870° C on heating seemed to be related to the incongruent melting and two exothermic peaks at 820 and 810° C due to crystallization were also observed cooling. Because the X-ray powder diffraction patterns of the sample agreed with those of $K_6Ti_4O_{11}$, the crystallization temperature of $K_6Ti_4O_{11}$ was determined to be 810° C. On the other hand, no typical peaks corresponding to $K_2Ti_2O_5$ were observed in the TG–DTA curve (b).

In samples I and II, successive weight losses were found below 800° C. The weight loss observed below 200° C corresponded to the desorption of water on the individual grain surfaces of the amorphous phase. On the basis of thermal weight loss, it is estimated that the amount of structural or adsorbed H_2O in amorphous materials was 2 mol per $K_2Ti_4O_9$ for sample I and 3.5 mol per $K_2Ti_4O_9$ for sample II, respectively.

The peaks at 1100° C observed in both amorphous samples corresponded to the melting of $K_2Ti_4O_9$ (the value given by Fujiki *et al.* [8] was 1100° C). On further heating above 1100° C, the weight loss progressed with the partial dispersion of K_2O from the chemical composition system. Only in the case of TG–DTA curve (b) was an endothermic peak observed at 1340° C. This was certainly due to the melting of $K_2Ti_6O_{13}$.

In order to understand the thermal profile mentioned above, X-ray diffraction measurements were carried out on both amorphous samples treated at 100, 400, 700, 1000 and 1350° C. These results are shown in Fig. 2. As seen in the figure, both amorphous materials of sample I (Fig. 2a) began to crystallize above 700° C after 3 h, and then were converted to the $K_2Ti_6O_{13}$ phase above 1100° C. Fig. 3 shows scanning electron micrographs of amorphous phases of (a)

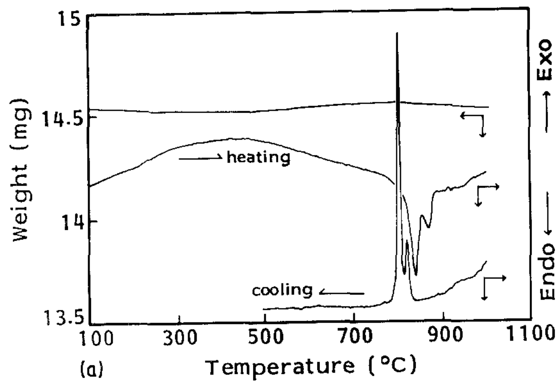

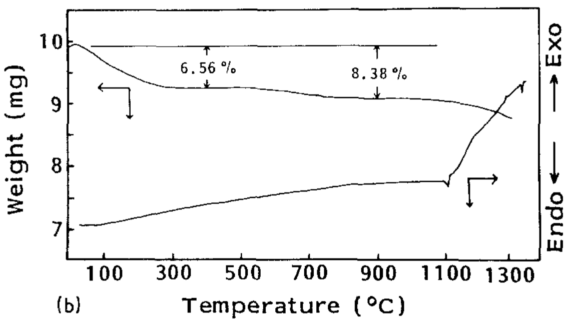

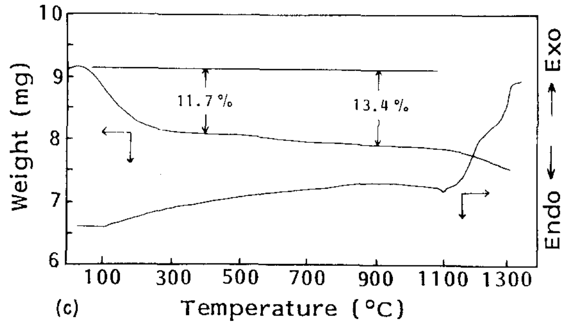

Figure 1 TG–DTA curves of potassium titanates. (a) Sample B, (b) sample I, (c) sample II.

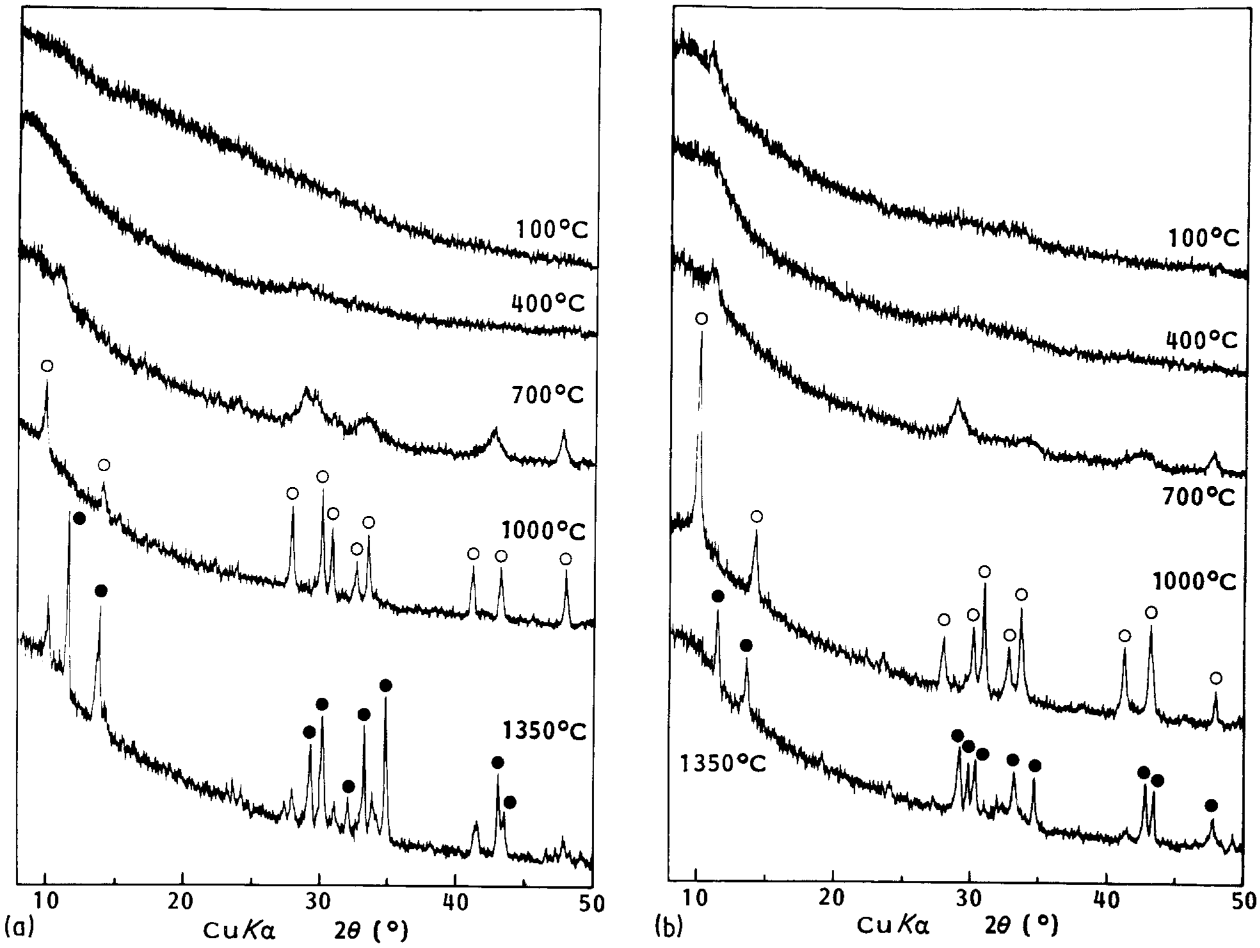

Figure 2 X-ray powder diffraction patterns of products calcined at various temperature. (a) Sample I, (b) sample II. (○) $K_2Ti_4O_9$, (●) $K_2Ti_6O_{13}$.

sample I and (b) sample II. Platelet and blocky grains were partly observed, but most grains appeared to form irregular shapes of different size. The scanning electron micrograph of amorphous materials (sample III) obtained from $K_2Ti_2O_5$ also showed the same grain shape, as seen in Fig. 3.

3.3. Characteristics of sintered potassium titanates

Figs 4a and b show the scanning electron micrographs of the fracture surface of sintered samples, which were moulded at 100 MPa and fired at 1000° C for 12 h using samples I and III as the starting materials. It should be noted that both amorphous starting samples were prepared using a platinum crucible. On heating, shrinkage of the sintered body was found to be ~75% of the original volume in case of sample I, but little shrinkage occurred when sample III was used as the starting powder. In the case of sample I, $K_2Ti_4O_9$ crystallized, retaining the shape of the amorphous phase with no change in the characteristic morphology. In case of sample II, $K_2Ti_4O_9$ in rectangular and platelet shapes was grown in the sintered body. In the case of sample III, needle-like crystals of $K_2Ti_4O_9$ were well grown and became entangled. On the basis of these observations, a sintered body was fabricated using a mixture of sample I and sample III as the starting materials. Fig. 5a shows the scanning electron micrograph of the fracture surface, which indicated that the reaction sintering could form the same crystalline phase and microstructure as the sintered body fabricated using sample II, as shown in

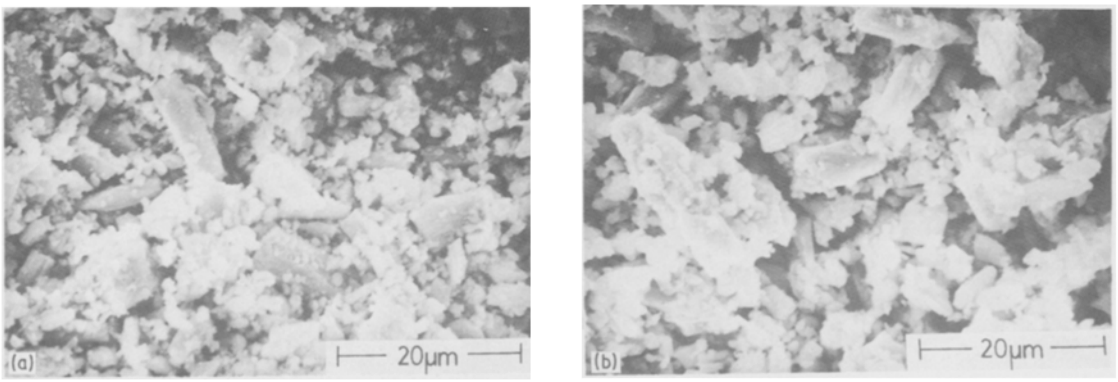

Figure 3 Scanning electron micrographs of amorphous powders. (a) Sample I, (b) sample II.

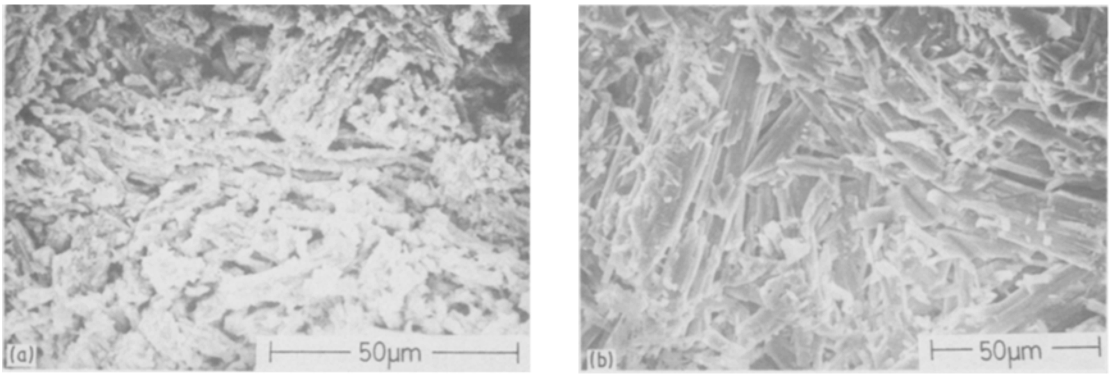

Figure 4 Scanning electron micrographs of the fracture surface of $K_2Ti_4O_9$ sintered bodies. (a)Sample I, (b) sample III.

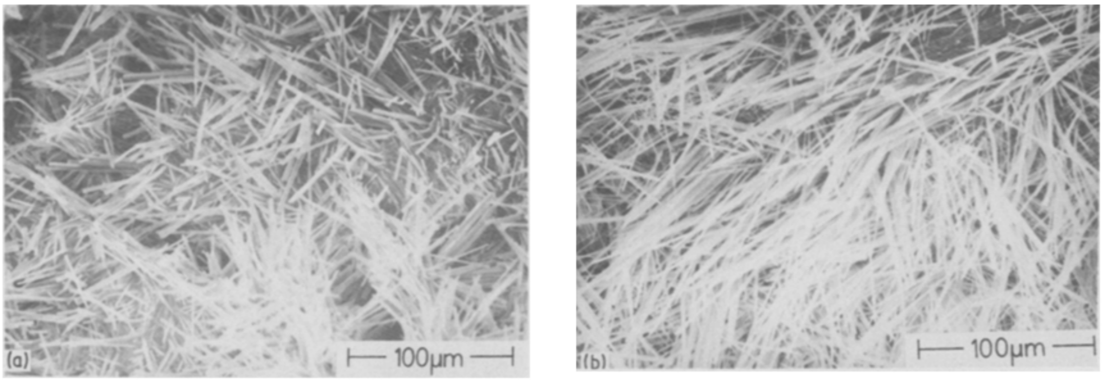

Figure 5 Scanning electron micrographs of the fracture surface of $K_2Ti_4O_9$ sintered bodies. (a) The mixture of samples I and III, (b) sample II.

Fig. 5b. The elongation of fibrous crystals appeared to be promoted by the thermal gradient between the interior and exterior of the sintering body and by the uniaxial pressure gradient induced on making the pellet.

The moulding pressure dependence of the relative density for sintered bodies of $K_2Ti_4O_9$ is shown in Fig. 6. The sintered body obtained using sample I as the starting material was sufficiently sintered and its relative density was about 90%. On the other hand, the sintered body obtained using sample II as the starting material did not shrink enough and its relative density was limited to ~70%. The difference in the relative density as shown in this figure depended strongly on the desorption quantity of water from the surface of the amorphous phases. As seen in Fig. 5, individual fibres of $K_2Ti_4O_9$ in the sintered body were combined with each other even when the sintered body had a low relative density, 44% at 50 MPa of the moulding pressure.

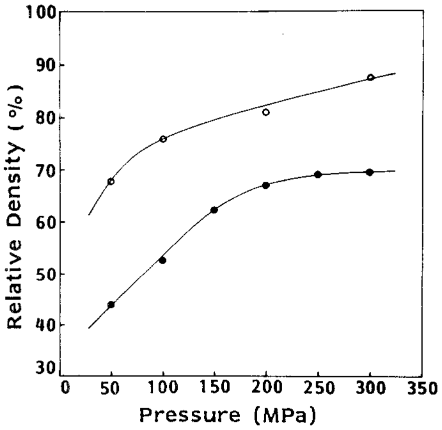

Figure 6 The moulding pressure dependence of the relative density for $K_2Ti_4O_9$ sintered bodies prepared using (○) sample I and (●) sample II.

In order to obtain a sintered body having a larger porosity, PVA(poly vinyl alcohol) was added into sample II in the proportion of 10 and 20 wt % and moulded at 200 MPa. Fig. 7 shows the scanning electron micrograph of the sample fabricated at 1000° C for 12 h. In this figure, some large hollows were locally observed, which were formed as a result of PVA being completely burned out after graphitization. In addition, it was found that the addition of PVA produced no change in the shape of the $K_2Ti_4O_9$ fibre texture. It was expected that the porosity was controlled by the amount of PVA added. In the present experiments, the relative densities of the sintered samples were 60% and 48% at 10 and 20 wt % PVA addition, respectively.

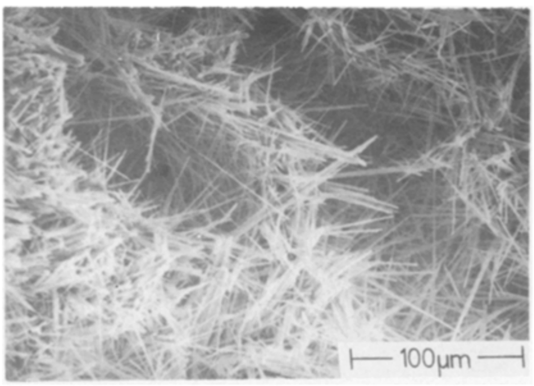

Figure 7 Scanning electron micrograph of the microstructure of $K_2Ti_4O_9$ sintered body with 20 wt % PVA.

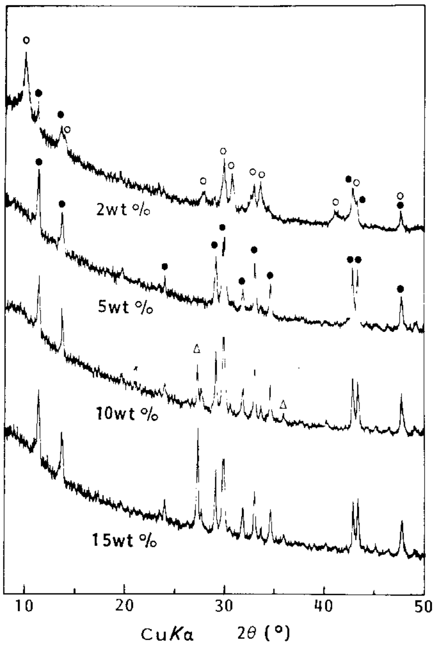

Figure 8 X-ray powder diffraction patterns of products calcined by the addition of various amounts of B_2O_3 at 1000° C. (○) $K_2Ti_4O_9$, (●) $K_2Ti_6O_{13}$, (△) TiO_2 (rutile).

As shown in Fig. 2, $K_2Ti_6O_{13}$ was formed above 1100° C, but its fibre or whisker shape was hardly maintained because the formation of $K_2Ti_6O_{13}$ progressed through the melting of $K_2Ti_4O_9$. B_2O_3 was added in the proportion 2, 5, 10 and 15 wt % to sample II and fired at 1000° C for 12 h. The X-ray powder diffraction patterns of the products are shown in Fig. 8. With increasing amount of B_2O_3, the intensity of the peaks corresponding to $K_2Ti_6O_{13}$ became stronger and the peaks identified as TiO_2 (rutile) were more frequently observed. This implied that $K_2Ti_6O_{13}$ was formed at 1000° C by the consumption of potassium ions from the amorphous materials because of the addition of B_2O_3.

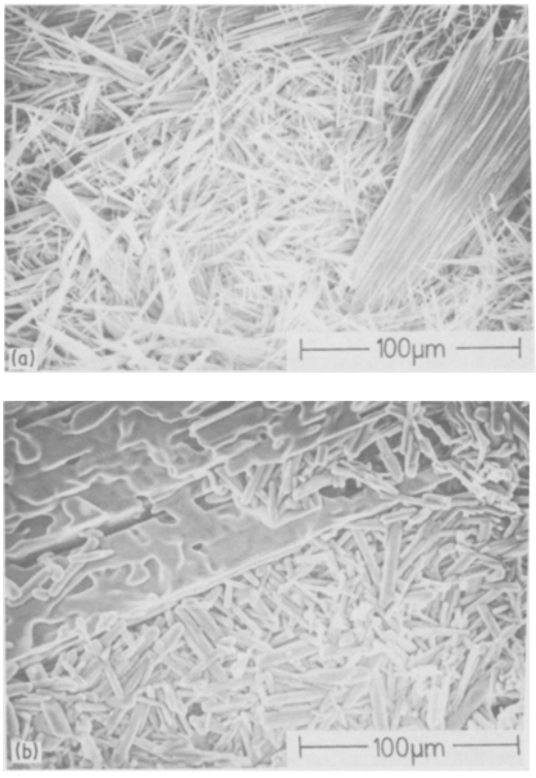

Figure 9 Scanning electron micrographs of the fracture surface of sintered bodies. (a) $K_2Ti_6O_{13}$, (b) $K_2Ti_6O_{13}$ + TiO_2 (rutile).

Fig. 9 shows the microstructures of sintered bodies prepared by the addition of (a) 5 wt % and (b) 15 wt % B_2O_3. As seen in the figure, the crystals in fibrous or bar-like shape were well grown and intertwined with each other depending on the B_2O_3 content. It is considered that the sintered body of $K_2Ti_6O_{13}$ with the porous microstructure was obtained by topotactic reaction from the fibrous crystal of $K_2Ti_4O_9$. It is estimated that the microstructure of the sintered body was intrinsically controlled by the amount of B_2O_3 and the reaction temperature. We conclude that the sintered body of fibrous $K_2Ti_6O_{13}$ crystals with a porous microstructure was fabricated by the experimental procedure described above.

4. Conclusions

1. A sintered body of $K_2Ti_4O_9$ with fibrous crystals intertwined was fabricated using amorphous phases as the starting materials, which were prepared by the leaching of the mixed phases of $K_2Ti_2O_5$ and $K_6Ti_4O_{11}$.
2. The porosity of the sintered body was controlled by the addition of PVA to the amorphous phases.
3. The sintered body of $K_2Ti_6O_{13}$, which consisted of fibrous crystals, was prepared by the addition of B_2O_3 to amorphous phases on heating at 1000° C for 12 h.

Acknowledgements

The authors thank Dr K. Nishiuti and Mr M. Suzue, Otsuka Chemical Co., for fruitful discussions. This work was partly supported by the grants of Otsuka Chemical Co.

References

1. A. J. EASTEAL and D. J. UDY, *High Temp. Sci.* **4** (1972) 487.
2. *Idem, J. Mater. Sci.* **8** (1973) 1171.
3. K. L. BERRY, V. D. AFTANDILIAN, W. W. GILBERT, E. P. H. MEIBOHM and H. S. YOUNG, *J. Inorg. Nucl. Chem.* **14** (1960) 231.
4. H. CID-DRESDNER and M. J. BUERGER, *Z. Kristallogr.* **117** (1962) 411.
5. T. ENDO, H. NAGAYAMA, T. SATO and M. SHIMADA, *J. Crystal Growth* **78** (1986) 423.
6. T. SHIMIZU, K. HASHIMOTO and H. YANAGIDA, *Yogyo-kyokai-shi* **84** (1976) 36.
7. Y. FUJIKI and T. OHSAKA, *ibid.* **90** (1982) 27.
8. Y. FUJIKI, F. IZUMI, T. OHSAKA and M. WATANABE, *ibid.* **85** (1977) 475.

Received 5 May
and accepted 20 July 1987